International Journal of Heat and Mass Transfer 52 (2009) 4350–4357

Contents lists available at ScienceDirect

International Journal of Heat and Mass Transfer

journal homepage: www.elsevier.com/locate/ijhmt

Optimal porosity distribution of fibrous insulation

Ning Du [a,b], Jintu Fan [a,*], Huijun Wu [a], Weiwei Sun [c]

[a] Institute of Textiles and Clothing, The Hong Kong Polytechnic University, Hong Kong
[b] School of Mathematics, Shandong University, Jinan 250100, China
[c] Department of Mathematics, City University of Hong Kong, Hong Kong

ARTICLE INFO

Article history:
Received 13 January 2008
Received in revised form 16 March 2009
Accepted 31 March 2009
Available online 15 May 2009

Keywords:
Porosity
Porous media
Conduction
Radiation
Insulation
Optimization

ABSTRACT

The porosity of fibrous materials is an important factor to their insulating performance. This paper considers the optimal porosity distribution of non-uniform fibrous porous medias for thermal insulation. Heat flow through the fibrous porous media is described by a coupled conduction–radiation heat transfer model which is numerically solved by using Finite Volume Method, and the optimal porosity distribution corresponding to the minimum total heat transfer is derived by applying a BFGS quasi-Newton optimization procedure. Variable analysis shows that the optimal porosity distribution is typically piecewise in conductive heat transfer dominated porous medium. For practical reasons, the change of porosity distribution across the thickness of the fibrous porous media may need to be continuous. To derive such a continuous optimal porosity distribution, a small penalty item should be introduced into the objective function. The study shows that, a continuous optimal porosity distribution generally has relatively high porosity at both boundaries and relatively low porosity in the centre region. The optimal distribution depends on many factors such as fibre radius, fibre emissivity, temperature difference, and overall mean porosity.

1. Introduction

It is well known that the porosity or fibre fractional volume is an important factor to the thermal insulating performance of fibrous porous materials [1–6]. Although there are other parameters of porous structures, such as pore diameter and pore shape which can also affect the thermal resistance, we concentrate on the effect of porosity distribution at present. Nevertheless, the question whether there is an optimal distribution of porosity, and which form this distribution of porosity should have are still not properly addressed. In [7], we showed that there is an optimal porosity for a uniform fibrous insulation in view of maximizing its thermal insulating performance, and proposed the use of Simulated Annealing Method for determining the optimal porosities of the constituent layers of a multi-layer fibrous insulation. Simulated Annealing Method may be appropriate for a multi-layer fibrous insulation consisting of a limited number of layers, it is inefficient and inadequate when dealing with the porosity distribution of a non-uniform fibrous insulation. The objective of the present study is to derive the optimal porosity distribution of a non-uniform fibrous insulation corresponding to the minimum total heat transfer and investigate how material and boundary parameters affect the distribution. A BFGS quasi-Newton optimization procedure is applied in this study.

2. Heat transfer model and optimization analysis

Consider a fibrous porous media of a fibrous material of thickness D held between the two plates at temperatures T_0 and T_D ($T_0 > T_D$). It has been shown in [1] that heat transfer within the fibrous material takes place by radiation and conduction, and convection can be neglected up to a porosity of 0.992.

Let x be the distance from the hot plate. Suppose the fibrous porous media is composed of randomly oriented fibres of radius R, and thermal emissivity e. Denote by $f(x)$ the fractional volume of fibre at point x, $\varepsilon(x) = 1 - f(x)$ the porosity distribution of the fibrous porous media. Consider a volume element of thickness dx at point x within the sample. Let $F_R(x)$ be the total thermal radiation incident on this volume element traveling to the right, $F_L(x)$ be the corresponding flux to the left. Ignoring the scattering of radiation by the fibres, the attenuation of the radiation fluxes is given by [1].

$$\frac{dF_R(x)}{dx} = -\beta(x)F_R(x) + \beta(x)\sigma T^4(x), \tag{1}$$

$$\frac{dF_L(x)}{dx} = \beta(x)F_L(x) - \beta(x)\sigma T^4(x), \tag{2}$$

where the absorption and emissivity coefficient $\beta(x) = \frac{f(x)e}{R}$.

* Corresponding author. Tel.: +852 2766 6472; fax: +852 2773 1432.
E-mail address: tcfanjt@inet.polyu.edu.hk (J. Fan).

0017-9310/$ - see front matter © 2009 Elsevier Ltd. All rights reserved.
doi:10.1016/j.ijheatmasstransfer.2009.03.067

Nomenclature

D	thickness of fibrous material (cm)
e, e_1, e_2	emissivity
f	fractional volume of fibre
F_L	thermal radiation to the left (W/m^2)
F_R	thermal radiation to the right (W/m^2)
H	Hessian matrix
I_{n1}, I_{n2}	subsets
k	effective thermal conductivity (W/m K)
k_a	thermal conductivity of air (W/m K)
k_f	thermal conductivity of fibre (W/m K)
N	number of layers
Q	total heat flow (W/m^2)
R	radius of fibres (μm)
x	position
T, T_0, T_D	temperature (K)

Greek symbols

β	absorption and emissivity coefficient
$\delta x, \Delta x$	distances of intervals
ε	porosity
$\varepsilon_*, \varepsilon^*$	lower and upper bound of porosity
$\bar{\varepsilon}$	mean porosity
γ	smoothing number
Υ	penalty number
η	improvement rates
λ	Lagrange multiplier
θ	angle (rad.)
σ	Boltzman constant (W/m^2 K^4)

Suppose the convective heat transfer is negligible and we only need to consider conductive and radiative heat transfer in the fibrous porous media, the total heat flow at point x is

$$Q = -k(x)\frac{dT(x)}{dx} + F_R(x) - F_L(x), \tag{3}$$

where $-k(x)\frac{dT(x)}{dx}$ stands for the conductive heat flow, $F_R(x) - F_L(x)$ stands for the radiative heat flow, and $k(x)$ is the effective thermal conductivity $k(x) = \varepsilon(x)k_a + f(x)k_f$.

At steady state condition, Q must be a constant and its derivative zero, so that Eq. (3) becomes

$$\frac{d}{dx}\left(k(x)\frac{dT(x)}{dx}\right) = \frac{dF_R(x)}{dx} - \frac{dF_L(x)}{dx}. \tag{4}$$

Boundary conditions are also needed. For temperature T, it is simply

$$T(0) = T_0, \quad T(D) = T_D, \tag{5}$$

for radiative heat flow, they are

$$(1 - e_1)F_L(0) + e_1\sigma T_0^4 = F_R(0), \tag{6}$$

$$(1 - e_2)F_R(D) + e_2\sigma T_D^4 = F_L(D). \tag{7}$$

In practice, the porosity value cannot be too high to introduce natural convection, or too small to reduce the permeability of the fibrous porous media to an unacceptably low value. Consequently, there are limits that the porosity values can change, viz. $0 < \varepsilon_* \leqslant \varepsilon(x) \leqslant \varepsilon^* < 1$, where ε_* and ε^* are the lower and upper bound of porosity values, respectively.

When the porosity distribution is isotropic, i.e., $\varepsilon = \varepsilon(x)$ holds constant, an analytical optimal porosity is derived in [7]

$$\varepsilon = 1 - \sqrt{\frac{8\sigma\bar{T}^3R}{e(k_f - k_a)}}, \tag{8}$$

where $\bar{T} = (T_0 + T_D)/2$, and (8) can be viewed as the optimal porosity distribution of the single-layer case.

Given different distribution of porosity $\varepsilon(x)$ with the other parameters unchanged, the heat transfer model (1)–(7) will result in different total heat loss Q. Therefore, Q can be viewed as a functional of $\varepsilon(x)$ so that the fundamental optimization problem is to find an optimal porosity distribution $\varepsilon = \varepsilon(x)$ such that

$$\begin{aligned} &\min_{\varepsilon(x)} \quad Q(\varepsilon) \\ &\text{s.t.} \quad 0 < \varepsilon_* \leqslant \varepsilon(x) \leqslant \varepsilon^* < 1. \end{aligned} \tag{9}$$

Sometimes, it may also be necessary to keep the overall mass of the fibrous porous media (in other words, fixing the overall mean porosity $\bar{\varepsilon}$) constant and to seek the maximal thermal insulation by merely changing its geometric structure, hence the optimization problem becomes

$$\begin{aligned} &\min_{\varepsilon(x)} \quad Q(\varepsilon) \\ &\text{s.t.} \quad 0 < \varepsilon_* \leqslant \varepsilon(x) \leqslant \varepsilon^* < 1, \\ &\qquad \int_0^D \varepsilon(x)dx = D\bar{\varepsilon}. \end{aligned} \tag{10}$$

Since it is hard to obtain the analytical expression of $Q(\varepsilon)$ from the heat transfer model (1)–(7), we consider a simple case with radiation heat being ignored (reasonable for fibrous porous media with relatively lower porosity, where conductive heat is the dominating part), hence

$$\frac{d}{dx}\left(k(x)\frac{dT(x)}{dx}\right) = 0. \tag{11}$$

It is easy to determine in this case the total heat $Q = \frac{T_0 - T_D}{\int_0^D 1/k(x)\,dx}$, so the optimization problem is to find the optimal porosity distribution $\varepsilon = \varepsilon(x)$ such that $\min_{\varepsilon(x)} Q(\varepsilon)$, which is identical to $\max_{\varepsilon(x)} \int_0^D \frac{1}{k(x)}dx$. Set $\varepsilon(x) = \varepsilon_* + (\varepsilon^* - \varepsilon_*)\sin^2\theta(x)$, we have

$$\begin{aligned} \int_0^D \frac{1}{k(x)}dx &= \int_0^D \frac{1}{(k_a - k_f)(\varepsilon_* + (\varepsilon^* - \varepsilon_*)\sin^2\theta(x)) + k_f}dx \\ &= \int_0^D F(x,\theta)dx. \end{aligned} \tag{12}$$

Euler equation in variational analysis [8] shows

$$\frac{dF}{d\theta} = -\frac{(k_a - k_f)(\varepsilon^* - \varepsilon_*)\sin 2\theta(x)}{\left((k_a - k_f)(\varepsilon_* + (\varepsilon^* - \varepsilon_*)\sin^2\theta(x)) + k_f\right)^2} = 0,$$

which gives $\theta(x) = n\pi/2$ $(n = 0, \pm1, \pm2, \ldots)$, corresponding to $\varepsilon(x) \equiv \varepsilon^*$ or $\varepsilon(x) \equiv \varepsilon_*$. This is easily understandable, since without radiation, maximal conductive heat takes place when $\varepsilon(x) \equiv \varepsilon_*$ and minimum takes place when $\varepsilon(x) \equiv \varepsilon^*$.

When the constraint $\int_0^D \varepsilon(x)dx = D\bar{\varepsilon}$ applies, an Lagrange multiplier λ may be introduced into the objective functional to give

$$\begin{aligned} \int_0^D F(x,\theta,\lambda)dx = &\int_0^D \frac{1}{(k_a - k_f)(\varepsilon_* + (\varepsilon^* - \varepsilon_*)\sin^2\theta(x)) + k_f}dx \\ &+ \lambda\left(\int_0^D \sin^2\theta(x)dx - \frac{D\bar{\varepsilon} - D\varepsilon_*}{\varepsilon^* - \varepsilon_*}\right). \end{aligned} \tag{13}$$

In this case, Euler equation shows

$$\begin{cases} \frac{dF}{d\theta} = -\frac{(k_a-k_f)(\varepsilon^*-\varepsilon_*)\sin 2\theta(x)}{\left((k_a-k_f)\left(\varepsilon_*+(\varepsilon^*-\varepsilon_*)\sin^2\theta(x)\right)+k_f\right)^2} + \lambda \sin 2\theta(x) = 0, \\ \frac{dF}{d\lambda} = \int_0^D \sin^2\theta(x)dx - \frac{D\bar{\varepsilon}-D\varepsilon_*}{\varepsilon^*-\varepsilon_*} = 0. \end{cases}$$

The only analytical solution of the above equations is $\sin^2\theta(x) = \frac{\bar{\varepsilon}-\varepsilon_*}{\varepsilon^*-\varepsilon_*}$, viz., $\varepsilon(x) \equiv \bar{\varepsilon}$. Under this porosity distribution, the heat transfer is maximum. This implies that the continuous optimal model (10) may not have any minimal solution, since the Euler's method requires that the solution is smooth, the optimal heat transfer problem achieves its minimum at a non-smooth point.

Now we study a discrete model by assuming the non-uniform batting consisting of n layers of thickness Δx with a constant porosity at each layer. The integral in (12) can be rewritten by

$$\int_0^D \frac{1}{k(x)}dx = \Delta x \sum_{i=1}^n \frac{1}{k_i},$$

where $k_i = (k_a - k_f)\varepsilon_i + k_f$. When the porosity ε is continuous, the right-hand side in above equation can be considered as an approximation of this integral by using the mid-point rule. The corresponding constraint of equality in (10) is given by

$$\Delta x \sum_{i=1}^n \varepsilon_i = D\bar{\varepsilon}$$

so that the discrete optimization problem is described by

$$\begin{aligned} \max_{\varepsilon} \quad & P(\varepsilon) = \Delta x \sum_{i=1}^n \tfrac{1}{k_i} \\ \text{s.t.} \quad & 0 < \varepsilon_* \leqslant \varepsilon_i \leqslant \varepsilon^* < 1, \quad i = 1,2,\ldots,n, \\ & \Delta x \sum_{i=1}^n \varepsilon_i = D\bar{\varepsilon}. \end{aligned} \tag{14}$$

Similarly to the continuous counterpart, in terms of the method of Lagrange multiplier, we can show that the above maximation problem does not have any smooth solution, and the optimal solution is achieved only on the boundary. Assume

$$\varepsilon_i = \varepsilon_* \text{ for } i \in I_{n1} \quad \text{and} \quad \varepsilon_i = \varepsilon^* \text{ for } i \in I_{n2},$$

where I_{n1} and I_{n2} are two subsets of $I_n = \{1, 2, \ldots, n\}$, and $I_{n1} \bigcap I_{n2} = \emptyset$. Then the optimal problem (14) reduces to

$$\begin{aligned} \max_{\varepsilon} \quad & P(\varepsilon) = \Delta x \sum_{i\notin I_{n1}, i\notin I_{n2}} \tfrac{1}{k_i} + C_I \\ \text{s.t.} \quad & 0 < \varepsilon_* \leqslant \varepsilon_i \leqslant \varepsilon^* < 1, \quad i \notin I_{n1}, \quad i \notin I_{n2} \\ & \Delta x \sum_{i\notin I_{n1}, i\notin I_{n2}} \varepsilon_i = D\bar{\varepsilon} - \bar{\varepsilon}_I, \end{aligned} \tag{15}$$

where

$$\begin{aligned} C_I &= \Delta x\left(\sum_{i\in I_{n1}} \frac{1}{(k_a-k_f)\varepsilon_* + k_f} + \sum_{i\in I_{n2}} \frac{1}{(k_a-k_f)\varepsilon^* + k_f}\right), \\ \bar{\varepsilon}_I &= \Delta x\left(\sum_{i\in I_{n1}} \varepsilon_* + \sum_{i\in I_{n2}} \varepsilon^*\right). \end{aligned} \tag{16}$$

It is obvious that the optimization problem (15) is equivalent to the model in (14), but with less variables. Using the above analysis again, the model finally reduces to a problem with two variables only. This problem can be easily solved by fixing one variable at boundary values (ε_* or ε^*) and determining the other using the constraint of equality.

Based on the above analysis, we come to a conclusion that the optimal porosity distribution of conductive heat insulation problem may have multiple solutions which are typically piecewise and tend to be congregated at both ends. This means that, in a media dominated with conductive heat transfer, the piecewise distribution of porosity with extreme values of either ε_* or ε^* (at most one exception) reduces heat transfer.

When both conductive and radiative heat are taken into consideration, it is difficult to give analytical solutions to the optimization problem (10) or its discrete model. In this case, our numerical experiments below show that the optimal porosity distributions are still piecewise and normally fluctuated. In practical applications, too fast fluctuation of porosity across a tiny thickness may not be realistic, as fibres have specific fineness and length and the porosity by its definition is a macroscale average of the volume of space over the total volume. In order to derive a continuous optimal porosity distribution, a small penalty can be introduced to the objective function, and the optimization problem becomes

$$\begin{aligned} \min_{\varepsilon(x)} \quad & Q(\varepsilon) + \gamma \textstyle\int_0^D (\varepsilon'(x))^2 dx \\ \text{s.t.} \quad & 0 < \varepsilon_* \leqslant \varepsilon(x) \leqslant \varepsilon^* < 1 \end{aligned} \tag{17}$$

and

$$\begin{aligned} \min_{\varepsilon(x)} \quad & Q(\varepsilon) + \gamma \textstyle\int_0^D (\varepsilon'(x))^2 dx \\ \text{s.t.} \quad & 0 < \varepsilon_* \leqslant \varepsilon(x) \leqslant \varepsilon^* < 1, \\ & \textstyle\int_0^D \varepsilon(x)dx = D\bar{\varepsilon}, \end{aligned} \tag{18}$$

where $\varepsilon'(x)$ stands for the derivative of $\varepsilon(x)$ and γ is a small positive number. When γ is taken to be zero, we get the original fluctuating porosity distribution.

3. Numerical calculation and optimization

3.1. Finite volume method for heat transfer model

Finite volume method [9] is applied to compute the numerical solution of the heat transfer model (1)–(7). Let N be a positive integer, $0 = \tilde{x}_0 < \tilde{x}_1 < \tilde{x}_2 < \cdots < \tilde{x}_N = D$ be a discretization of $[0, D]$ and $[\tilde{x}_{i-1}, \tilde{x}_i]$ represent the ith control volume, make sure to locate the interfaces where the discontinuity in the material properties occurs. The grid points $x_1, x_2, \ldots, x_N$ are placed at the centres of the control volumes, i.e., $x_i = (\tilde{x}_{i-1} + \tilde{x}_i)/2$, and the two boundary points $x_0 = 0$, $x_{N+1} = D$ are added in. The distances between interfaces and/or grid points are denoted by $\Delta x_i = \tilde{x}_i - \tilde{x}_{i-1}$, $\delta x_i = x_i - x_{i-1}$, $\delta x_i^- = \tilde{x}_{i-1} - x_{i-1}$, $\delta x_i^+ = x_i - \tilde{x}_{i-1}$. Denote $T_i = T(x_i)$, $i = 0, 1, \ldots, N+1$; $(F_R)_i = F_R(\tilde{x}_i)$, $i = 0, 1, \ldots, N$, and similar notations for F_L.

Suppose $\{T_0, T_1, \ldots, T_{N+1}\}$ has been given. Integrating Eq. (1) over interval $[\tilde{x}_{i-1}, \tilde{x}_i]$ and using mid-point quadrature formula for the right-hand terms, we can obtain

$$(F_R)_i = \frac{2-\beta_i\Delta x_i}{2+\beta_i\Delta x_i}(F_R)_{i-1} + \frac{2\beta_i\Delta x_i\sigma T_i^4}{2+\beta_i\Delta x_i}, \quad i = 1,2,\ldots,N. \tag{19}$$

Similarly, for Eq. (2), we have

$$(F_L)_{i-1} = \frac{2-\beta_i\Delta x_i}{2+\beta_i\Delta x_i}(F_L)_i + \frac{2\beta_i\Delta x_i\sigma T_i^4}{2+\beta_i\Delta x_i}, \quad i = N, N-1, \ldots, 1. \tag{20}$$

The treatment of boundary conditions (6) and (7) is simple, viz.

$$(1-e_1)(F_L)_0 + e_1\sigma T_0^4 = (F_R)_0, \tag{21}$$

$$(1-e_2)(F_R)_N + e_2\sigma T_N^4 = (F_L)_N. \tag{22}$$

Schemes (8) and (9) show that the values of F_R can be computed forward, whereas F_L backward.

Denote by $\tilde{k}_{i-1}$ the heat conductivity at interface $\tilde{x}_{i-1}$, it can be determined by using the same strategy in [9]

$$\frac{\delta x_i}{\tilde{k}_{i-1}} = \frac{\delta x_i^-}{k_{i-1}} + \frac{\delta x_i^+}{k_i}. \tag{23}$$

Integrate Eq. (4) over the ith control volume $[\tilde{x}_{i-1}, \tilde{x}_i]$. Assume T is piecewise linear among the grid points, and denote $K_{i-1} = \frac{\tilde{k}_{i-1}}{\delta x_i}$, $K_i = \frac{\tilde{k}_i}{\delta x_{i+1}}$, we obtain the discrete scheme:

$$\begin{aligned} &K_{i-1}T_{i-1} - (K_{i-1} + K_i)T_i + K_iT_{i+1} \\ &= (F_R - F_L)_i - (F_R - F_L)_{i-1}, \quad i = 1, 2, \ldots, N. \end{aligned} \tag{24}$$

Note that the equations for $i = 1$ and $i = N$ should be modified using boundary conditions (5). Therefore, Eq. (13) become a tridiagonal system and can be solved by the efficient Thomas Algorithm [10]. After that, the updated values of $\{T_0, T_1, \ldots, T_{N+1}\}$ will be used in (8)–(11) for the next iteration step.

3.2. Discrete optimization problems and constraints handling

The temperature and radiation distribution $\{T_i\}, \{F_R\}, \{F_L\}$ $(i = 1, 2, \ldots, N)$ can be derived by the above numerical calculation of the heat transfer model. Apparently the total heat loss Q is a function of the discrete porosities, i.e., $Q = Q(\varepsilon_1, \varepsilon_2, \ldots, \varepsilon_N)$, and the discrete optimization problems become

$$\begin{aligned} \min_{(\varepsilon_1, \varepsilon_2, \ldots, \varepsilon_N)} \quad & Q(\varepsilon_1, \varepsilon_2, \ldots, \varepsilon_N) + \gamma \sum_{i=1}^{N-1} \left(\frac{\varepsilon_{i+1} - \varepsilon_i}{\Delta x_i}\right)^2 \Delta x_i \\ \text{s.t.} \quad & \varepsilon_* \leqslant \varepsilon_i \leqslant \varepsilon^*, \quad i = 1, \ldots, N \end{aligned} \tag{25}$$

and

$$\begin{aligned} \min_{(\varepsilon_1, \varepsilon_2, \ldots, \varepsilon_N)} \quad & Q(\varepsilon_1, \varepsilon_2, \ldots, \varepsilon_N) + \gamma \sum_{i=1}^{N-1} \left(\frac{\varepsilon_{i+1} - \varepsilon_i}{\Delta x_i}\right)^2 \Delta x_i \\ \text{s.t.} \quad & \varepsilon_* \leqslant \varepsilon_i \leqslant \varepsilon^*, \quad i = 1, \ldots, N \quad \text{(NEQC)} \\ & \bar{\varepsilon} = \tfrac{1}{N} \sum_{i=1}^{N} \varepsilon_i \quad \text{(EQC)} \end{aligned} \tag{26}$$

We concentrate on the optimization problem (26). In [7], Simulated Annealing method is conveniently used for the determination of optimal porosity distribution for 10-layers materials. Since we aim at finding if there exists any pattern of optimal porosity distribution in non-uniform fibrous porous media, materials with much more layers should be considered. The Simulated Annealing method is inadequate for this task due to its low convergence rate in solving high dimensional optimization problem. Therefore, the more efficient Quasi-Newton algorithm is adopted in the present study.

However, the Quasi-Newton algorithms are always used in solving unconstrained optimization. The constraints of inequalities (NEQC) and the equality (EQC) should be removed first.

To remove the inequality constraints (NEQC), we introduce the trigonometric substitution:

$$\varepsilon_i = \frac{\varepsilon^* + \varepsilon_*}{2} + \frac{\varepsilon^* - \varepsilon_*}{2} \sin\theta_i, \quad i = 1, \ldots, N. \tag{27}$$

Thus for arbitrary θ_i, the corresponding ε_i satisfies inequality constraints automatically.

The equality constraint (EQC) becomes

$$\sum_{i=1}^{N} \sin\theta_i = N \cdot \frac{2\varepsilon - \varepsilon^* - \varepsilon_*}{\varepsilon^* - \varepsilon_*} = \delta \tag{28}$$

and it can be treated by introducing another form of penalty item in the objective function:

$$\begin{aligned} J(\theta_1, \theta_2, \ldots, \theta_N) &= Q(\theta_1, \theta_2, \ldots, \theta_N) \\ &\quad + \gamma \sum_{i=1}^{N-1} \left(\frac{\sin\theta_{i+1} - \sin\theta_i}{\Delta x_i}\right)^2 \Delta x_i \\ &\quad + \Upsilon \left(\sum_{i=1}^{N} \sin\theta_i - \delta\right)^2, \end{aligned} \tag{29}$$

where Υ is a large positive number, which means unless the equality constraint is held, the penalty will be too large to give the optimal parameters. If Υ is taken to zero, it represent the optimization problem without equality constraint (25).

In summary, the final discrete optimization problem becomes

$$\min_{(\theta_1, \theta_2, \ldots, \theta_N)} J(\theta_1, \theta_2, \ldots, \theta_N) \tag{30}$$

with the parameters $(\theta_1, \theta_2, \ldots, \theta_N)$ unconstrained.

3.3. BFGS quasi-Newton method for optimization

Newton's method is well known for solving unconstrained nonlinear optimization problem due to its fast quadratic convergence. It uses the first and second derivatives (gradient and Hessian) to find the stationary point of the objective function $y = f(x)$, where x is a multi-dimensional vector:

$$x_{k+1} = x_k - H^{-1}(x_k)\nabla f(x_k), \tag{31}$$

where $\nabla f(x_k)$ and $H(x_k)$ are the gradient and the Hessian at x_k, respectively.

However, the evaluation of the Hessian or its inverse matrix is often impractical or very time-consuming. In Quasi-Newton methods, the Hessian matrix need not to be computed at any stage but to be updated typically by adding a simple low-rank update to the current estimate of the Hessian. The Broyden–Fletcher–Goldfarb–Shanno (BFGS) method is the most successful one in the Quasi-Newton algorithms, which has the form [11]

$$H_k^{-1} = H_{k-1}^{-1} - \frac{H_{k-1}^{-1} y_k s_k^T + s_k y_k^T H_{k-1}^{-1}}{y_k^T s_k} + \left(1 + \frac{y_k^T H_{k-1}^{-1} y_k}{s_k^T y_k}\right) \frac{s_k s_k^T}{s_k^T y_k}, \tag{32}$$

where $s_k = x_k - x_{k-1}$, $y_k = \nabla f(x_k) - \nabla f(x_{k-1})$, H_k^{-1} is the approximation of $H^{-1}(x_k)$.

After H_k^{-1} being updated from H_{k-1}^{-1}, it is obviously that $d_k = -H_k^{-1}\nabla f(x_k)$ is a descent direction and thus a 1D line search algorithm is needed to find an optimal α_k such that

$$x_{k+1} = x_k + \alpha_k d_k \quad \text{and} \quad f(x_{k+1}) = \min_{\alpha} f(x_k + \alpha d_k). \tag{33}$$

But in general, it is too expensive to identify the optimal value of α_k since it requires too many evaluations of the objective function f and its gradient ∇f, thus a more practical line search strategy based on cubic interpolation and backtracking approach [11,12] is introduced in the program to ensure sufficient decrease of the values of the objective function.

The penalty number Υ in objective function (25) cannot be too small, because a small Υ could not successfully reflect the penalty for disobeying the equality constraint. Yet a too large Υ may reduce accuracy in numerical computation. Consequently, an adaptive selection of Υ is proposed by using the Sequence Unconstrained Optimization Technique [13].

A brief description of BFGS Quasi-Newton algorithm is as follows:

1. Set initial values:
   $k = 0$; Initial guess x_0; Initial penalty coefficient σ; $H_0^{-1} = I$.
2. Evaluate $\nabla f(x_k)$ using finite-difference.
3. If $||\nabla f(x_k)|| \leqslant \varepsilon$, turn to Step 5.
   Otherwise:
   (1) Compute $d_k = -H_k^{-1}\nabla f(x_k)$.
   (2) Find suitable α_k by a line search algorithm.
   (3) Update x_{k+1} from (33).
4. $k = k + 1$; Update H_k^{-1} from (32); and turn to Step 2.
5. Compute the penalty related to the equality constraint, if small enough, stop.
   Otherwise: Set $\Upsilon = a\Upsilon$ $(a > 1)$, and turn to Step 2.

4. Optimal porosity distribution in non-uniform fibrous porous media

Consider a fibrous porous media held between hot and cold plates at different temperatures. Consider the fibrous porous media consists of N layers, each having its own porosity, viz. $\varepsilon_1, \varepsilon_2, \ldots, \varepsilon_N$. The other material parameters, such as emissivity e, fibre radius R and fibre conductivity k_f, etc. hold constant anywhere in the fibrous porous media. Given a small smoothing factor γ, the above numerical calculation and optimization procedure can be applied to give the discrete optimal porosity distribution of problems (25) and (26).

In the numerical experiments reported below, if not given specifically, the following parameters are used: $D = 3$ cm, $N = 500$, $T_0 = 35$ °C, $T_D = -20$ °C, $k_a = 0.025$ W/m K, $k_f = 0.2$ W/m K, $e_1 = e_2 = 0.6$, $e = 0.6$, $\varepsilon_* = 0.6$, $\varepsilon^* = 0.992$.

4.1. Experiments on optimization problem without fixed mean porosity constraint

Fig. 1(a)–(f) plot the optimal porosity distribution of problem (25) with different penalty coefficients $\gamma = 0, 0.001, 0.001, 0.01, 0.05, 0.1$. The fibre radius of the fibrous porous media is $R = 10$ μm. Table 1 shows the corresponding total heat transfer Q_γ and the improvement rates η in comparison with the total heat transfer Q_ε when $\varepsilon = 0.97$, the optimal porosity of the uniform fibrous porous media. η is calculated by

$$\eta = \frac{Q_\varepsilon - Q_\gamma}{Q_\varepsilon} \times 100\%. \tag{34}$$

It can be seen from the results that, the derived optimal porosity distribution exhibits oscillation when there is no smoothening ($\gamma = 0$) or the penalty coefficient is very small ($\gamma = 0.0001$), a continuous optimal porosity distribution can be obtained at a higher value of γ. Too high value of γ is however not appropriate as this would result in little improvement over the uniform fibrous porous media in terms of thermal insulation. Although the solution of continuous optimal porosity distribution depends on the penalty coefficient γ, the exact value of which is difficult to determine, there is a clear trend in terms of the shape of the continuous optimal porosity distribution. It is clear that oscillation of porosity across the thickness of the fibrous porous media is beneficial to thermal insulation. If smoothened continuous porosity distribution is required for practical reasons, in order to improve thermal insulation, the porosity should be higher at both ends and lower in the intermediate zone. This trend can be explained by the conductive and radiative heat flow across the thickness of the fibrous porous media (see Fig. 2 of [1]). The conductive heat flow is higher at both ends and lower at the intermediate zone, while the radiative heat flow is just in the opposite situation. Higher porosity at both ends can reduce the conductive heat transfer effectively and but only slightly increase radiative heat transfer, and hence reduce the overall heat loss. Another feature of the porosity curve is that, the turning point of the hot side is lower than that of the cold side. This is because radiative heat flow is proportional to the fourth power of temperature. Radiative heat flow is stronger at the hot side than that at the cold side and to reduce radiation, greater fibre volume fraction at the hot side can minimize radiative heat transfer.

Fig. 2(a)–(e) plots the optimal porosity distributions derived with varying fibre radius ($R = 1$, 2, 10, 20, 50 μm, respectively), by fixing the penalty coefficient $\gamma = 0.05$ and other material and boundary parameters.

It can be seen from these figures that, with increasing fibre radius R, the high porosity regions at both ends expand, the low porosity region in the centre shrinks, and the porosity value in the central region and its changing slope decrease. This phenomenon can be explained by the increased radiative heat flow and boundary effects with a smaller absorption constant β resulted from a greater fibre radius R. For coarser fibrous insulation, a non-uniform fibrous insulation with an optimal porosity distribution provides greater improvement over a uniform fibrous insulation (see Fig. 2(f)).

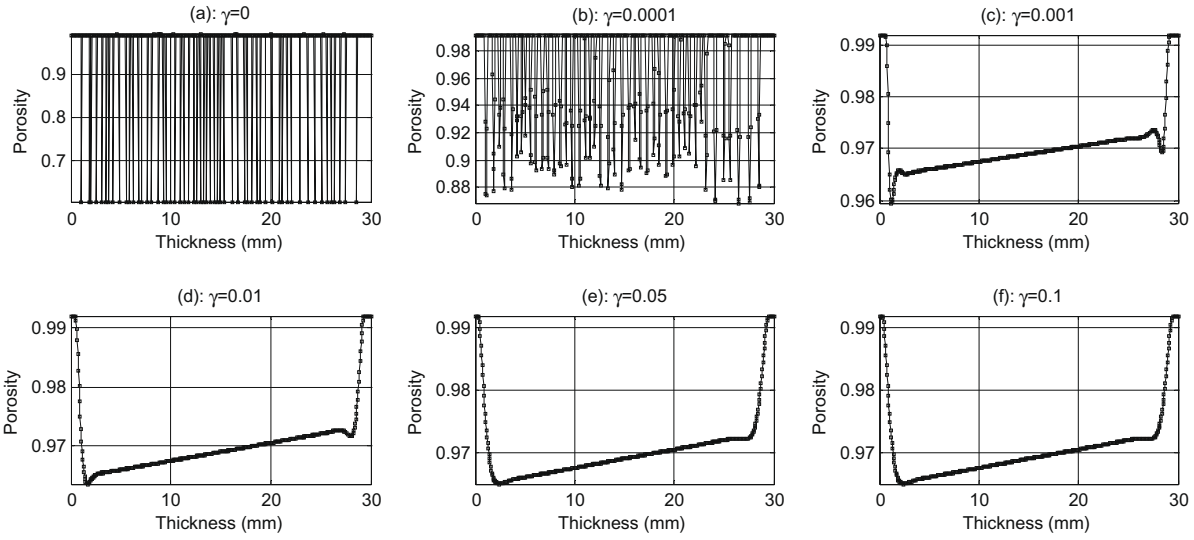

Fig. 1. Optimal porosity distributions with different penalty coefficients.

Table 1
Total heat transfer and improvement rates of different penalty coefficients.

	$\gamma = 0$	$\gamma = 0.0001$	$\gamma = 0.001$	$\gamma = 0.01$	$\gamma = 0.05$	$\gamma = 0.1$	$\varepsilon \equiv 0.97$
$Q_\gamma(Q_\varepsilon)$	59.003	63.534	65.013	65.021	65.035	65.047	65.486
η (%)	9.899	2.981	0.721	0.709	0.689	0.670	0.0

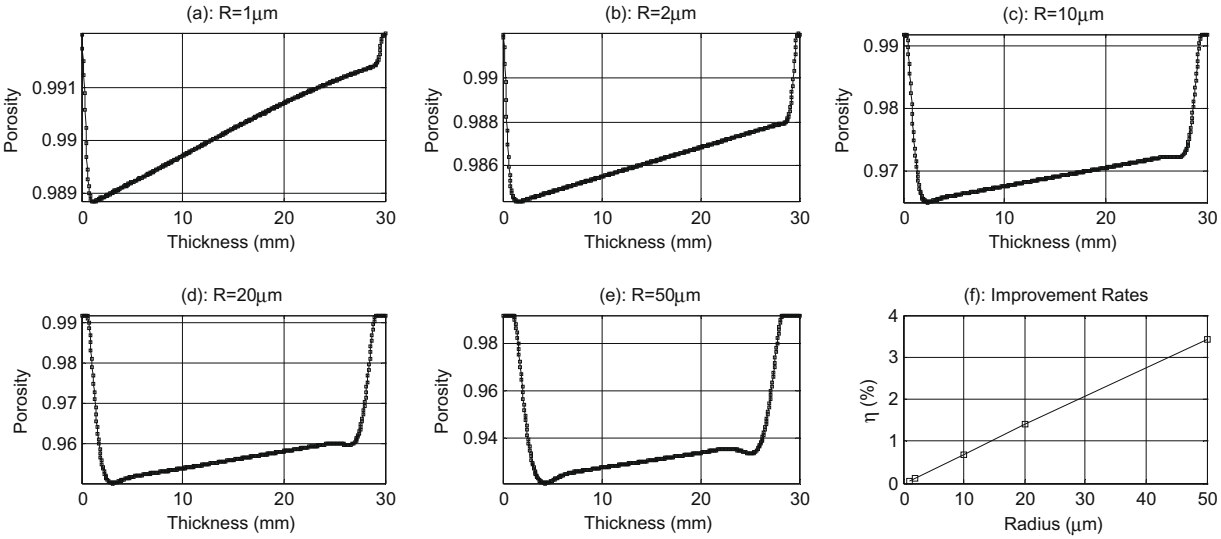

Fig. 2. Optimal porosity distributions with different fibre radius and their improvement rates.

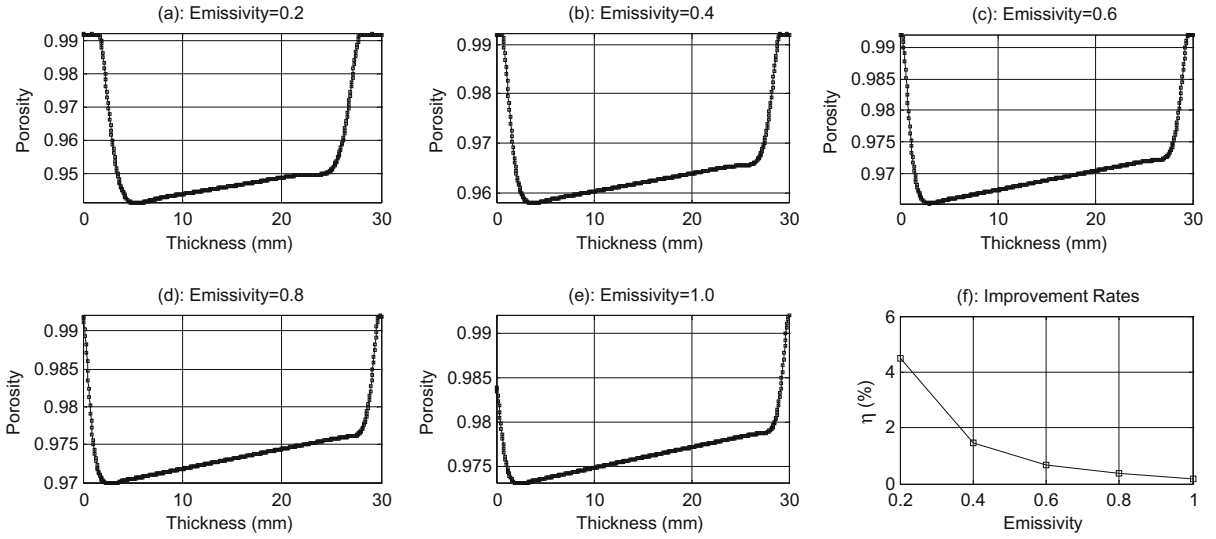

Fig. 3. Optimal porosity distributions with different fibre emissivity and their improvement rates.

Fig. 3(a)–(e) plots the effect of fibre emissivity on the optimal porosity distribution, with $e = 0.2$, 0.4, 0.6, 0.8, 1.0, respectively. Fig. 3(f) shows the improvement rates of thermal insulation with increasing fibre emissivity. It can be seen, for fibrous porous media consisting fibres of lower fibre emissivity, an optimal non-uniform porosity distribution gives greater improvements in thermal insulation in comparison with a uniform optimal porosity. This is understandable in view of the definition of the absorption constant $\beta = fe/R$. Lower emissivity means lower absorption constant and hence greater amount of radiative heat transfer, which can be reduced by an optimal non-uniform porosity distribution.

Fig. 4(a)–(e) shows the effects of temperatures of hot and cold sides on the optimal porosity distribution, with (1) $T_0 = 35$ °C, $T_D = -20$ °C, (2) $T_0 = 70$ °C, $T_D = -40$ °C, (3) $T_0 = 140$ °C, $T_D = -80$ °C, (4) $T_0 = 210$ °C, $T_D = -120$ °C (5) $T_0 = 350$ °C, $T_D = -200$ °C, respectively. The penalty coefficient $\gamma = 0.1$, fibre radius $R = 10$ μm, and the other parameters are the same as before. Fig. 4(f) plots the improvement rates of thermal insulation as a function of temperature difference.

It can be seen from these figures that, with the increase of temperature difference on both sides, for optimal thermal insulation, there should be a sharper decrease in porosity near the hot side,

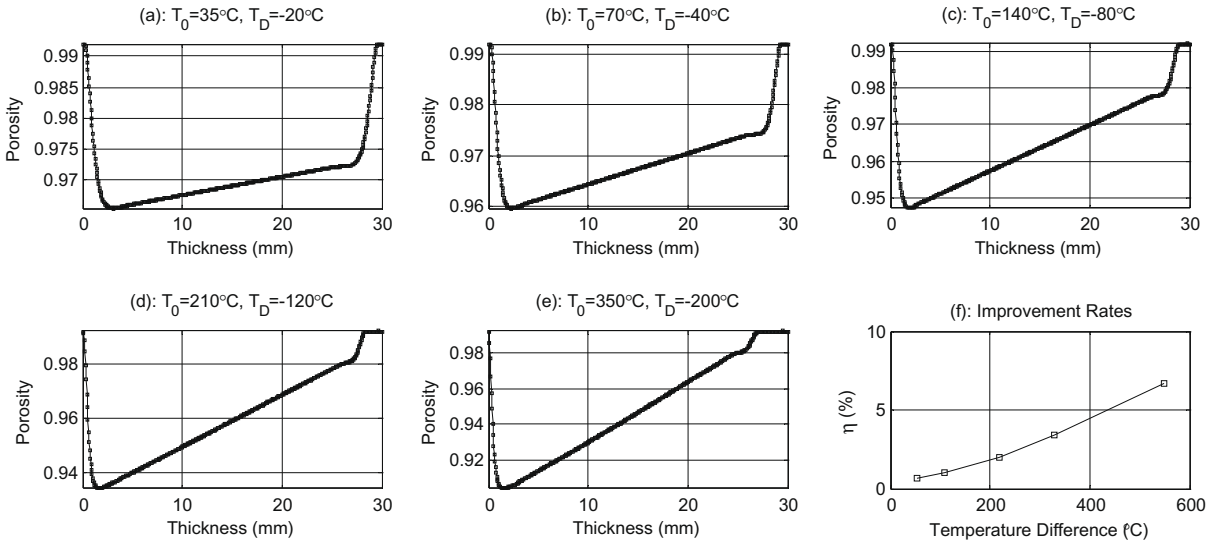

Fig. 4. Optimal porosity distributions with different temperature differences and their improvement rates.

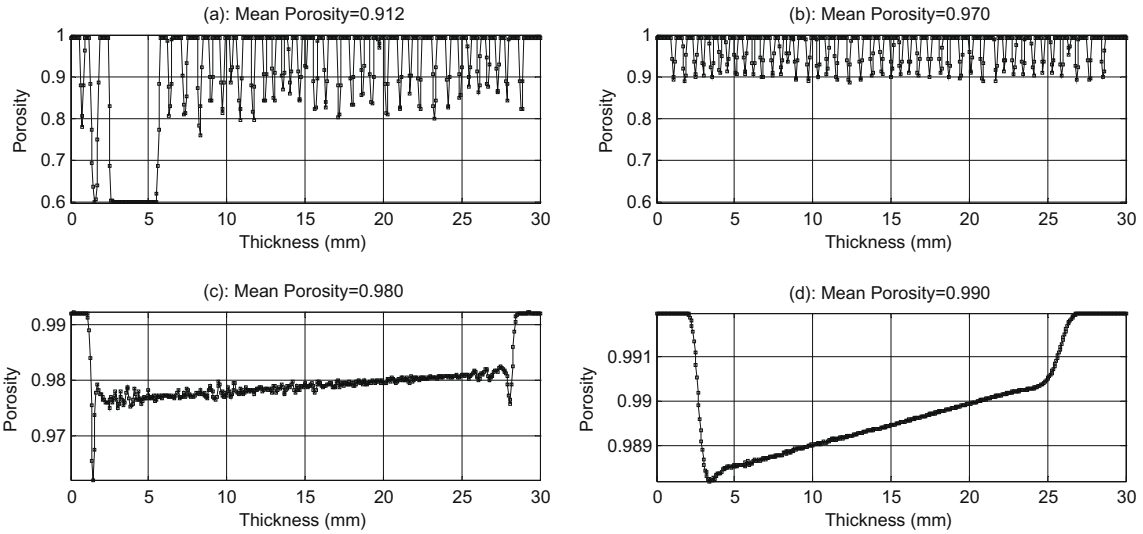

Fig. 5. Optimal porosity distributions with different mean porosity values.

and relatively higher porosity near the cold side. The slope of the intermediate zone becomes more inclined. It can also be explained by the fact that radiative heat transfer is proportional to the fourth power of temperature, and hence there is much great fraction of radiative heat transfer at the hot side.

4.2. Experiments on optimization problem with fixed mean porosity constraint

Fig. 5(a)–(d) compares the results of optimal porosity distribution with different mean porosity value, viz. $\bar{\varepsilon} = 0.912,\ 0.97, 0.98,\ 0.99$, respectively. The penalty coefficient $\gamma = 0.0001$, fibre radius $R = 10\ \mu m$, and the other parameters are the same as before. It is obviously that with the increase of the mean porosity value, the corresponding porosity distribution become more smooth, even the penalty coefficient γ is very small. Since larger mean porosity value represents higher ratio of thermal radiation and lower ratio of conductive heat in the total heat transfer, oscillation of porosity distribution have greater impact on the reduction of conductive heat, but little effect on the reduction of radiative heat.

5. Conclusions

In this paper, we consider the optimal porosity distribution of non-uniform fibrous porous media held between hot and cold plates in view of providing maximal thermal insulation. The mechanism of heat transfer is described by a conduction–radiation coupled model which is numerically computed by using Finite Volume Method. A BFGS Quasi-Newton procedure is employed for the determination of optimal porosity distribution for its high efficiency in optimization. Two kinds of optimization problems with or without fixed mean porosity constraint are considered. Different optimal porosity distribution are derived and compared, corresponding to different penalty coefficient, fibre radius, fibre emissivity, temperature difference, and different mean porosity value. The study show that piecewise distributed porosity within the fibrous media can significant reduce conductive heat transfer. If continuous porosity distribution is required for practical reasons, for optimal thermal insulation, the general pattern is higher porosity at both boundaries of the fibrous porous media and steadily increasing in the intermediate zone, which coincides with the

fraction of thermal radiation within the fibrous porous media. For fibrous insulation consisting of coarse fibres, fibres of lower surface emissivity and exposed to greater temperature difference, an optimal non-uniform porosity distribution can provide more significant improvements in thermal insulation in comparison with a uniform porosity distribution.

The algorithms of numerical simulation and optimization can be expected to apply into more sophisticated problems, e.g., the transient heat–moisture transfer model, to give the optimal porosity distribution of fibrous materials corresponding to a combined objective of minimal heat transfer and maximum moisture transfer.

Acknowledgements

The authors would like to thank the funding support of Research Grant Council of HKSAR (PolyU 5162/08E) and Hong Kong Polytechnic University (Project No. 1-BB82), the National Natural Science Foundation of China (Grant No. 10801092) and the National Basic Research Program of China (973 Program, Grant No. 2007CB814906).

References

[1] B. Farnworth, Mechanisms of heat flow through clothing insulation, Textile Research Journal 53 (12) (1983) 717–725.
[2] J. Fan, X. Cheng, X. Wen, W. Sun, An improved model of heat and moisture transfer with phase change and mobile condensates in fibrous insulation and comparison with experimental results, International Journal of Heat and Mass Transfer 47 (10&11) (2004) 2343–2352.
[3] H. Wu, J. Fan, N. Du, Thermal energy transport within porous polymer materials: effects of fiber parameters, Journal of Applied Polymer Science 106 (1) (2007) 576–583.
[4] J. Fan, X. Wen, Modelling heat and moisture transfer through fibrous insulation with phase change and mobile condensates, International Journal of Heat and Mass Transfer 45 (19) (2002) 4045–4055.
[5] X. Cheng, J. Fan, Simulation of heat and moisture transfer with phase change and mobile condensates in fibrous insulation, International Journal of Thermal Sciences 43 (7) (2004) 665–676.
[6] J. Fan, X. Cheng, Heat and moisture transfer with sorption and phase change through clothing assemblies, Part II: Theoretical modeling, simulation, and comparison with experimental results, Textile Research Journal 75 (3) (2005) 187–196.
[7] N. Du, J. Fan, H. Wu, Optimum porosity of fibrous porous materials for thermal insulation, Fibers and Polymers 9 (1) (2008) 27–33.
[8] D.R. Smith, Variational Methods in Optimization, Prentice-Hall, Englewood Cliffs, NJ, 1974.
[9] S.V. Patankar, Numerical Heat Transfer and Fluid Flow, Hemisphere, New York, 1980.
[10] J.D. Anderson, Computational Fluid Dynamics: The Basics with Applications, McGraw-Hill, New York, 1995.
[11] J. Nocedal, S.J. Wright, Numerical Optimization, Springer, New York, 1999.
[12] W.H. Press, S.A. Teukolsky, W.T. Vetterling, B.P. Flannery, Numerical Recipes in Fortran 77: The Art of Scientific Computing, Cambridge University Press, New York, 1992.
[13] A.V. Fiacco, G.P. McCormick, Computational algorithm for the sequential unconstrained minimization technique for nonlinear programming, Management Science 10 (4) (1964) 601–617.